Biomed Microdevices (2011) 13:973–982
DOI 10.1007/s10544-011-9567-x

Electrical detection of dsDNA and polymerase chain reaction amplification

Eric Salm · Yi-Shao Liu · Daniel Marchwiany · Dallas Morisette · Yiping He · Arun K. Bhunia · Rashid Bashir

Published online: 26 July 2011

Abstract Food-borne pathogens and food safety-related outbreaks have come to the forefront over recent years. Estimates on the annual cost of sicknesses, hospitalizations, and deaths run into the billions of dollars. There is a large body of research on detection of food-borne pathogens; however, the widely accepted current systems are limited by costly reagents, lengthy time to completion, and expensive equipment. Our aim is to develop a label-free method for determining a change in DNA concentration after a PCR assay. We first used impedance spectroscopy to characterize the change in concentration of purified DNA in deionized water within a microfluidic biochip. To adequately measure the change in DNA concentration in PCR solution, it was necessary to go through a purification and precipitation step to minimize the effects of primers, PCR reagents, and excess salts. It was then shown that the purification and precipitation of the fully amplified PCR reaction showed results similar to the control tests performed with DNA in deionized water. We believe that this work has brought label free electrical biosensors for PCR amplification one step closer to reality.

Keywords Label-free · Electrical detection · PCR · DNA · Listeria

E. Salm · R. Bashir
Department of Bioengineering,
University of Illinois at Urbana-Champaign,
Urbana, IL 61801, USA

E. Salm · D. Marchwiany · R. Bashir
Micro and Nanotechnology Laboratory,
University of Illinois at Urbana-Champaign,
Urbana, IL 61801, USA

D. Marchwiany
Department of Molecular and Cellular Biology,
University of Illinois at Urbana-Champaign,
Urbana, IL 61801, USA

Y.-S. Liu
Taiwan Semiconductor Manufacturing Corporation,
Hsinchu, Taiwan 300, Republic of China

D. Morisette
BioVitesse, Inc.,
West Lafayette, IN, USA

A. K. Bhunia
Department of Food Science, Purdue University,
West Lafayette, IN 47907, USA

Y. He
USDA-ARS-ERRC,
Wyndmoor, PA 19038, USA

R. Bashir (✉)
Department of Electrical and Computer Engineering,
University of Illinois at Urbana-Champaign,
Illinois, IL 61801, USA
e-mail: rbashir@illinois.edu

Present Address:
D. Morisette
Birck Nanotechnology Center, Purdue University,
West Lafayette, IN 47907, USA

1 Introduction

Food pathogens and food safety-related outbreaks have come to the forefront over recent years. From *Escherichia coli* O157:H7 in spinach to *Listeria monocytogenes* outbreaks in ready-to-eat deli meats, people have taken notice when it comes to keeping their food safe. The Centers for Disease Control and Prevention (CDC) estimates that there are 47.8 million cases of food-borne illnesses every year in the United States alone. Among those cases, 127,839 resulted in hospitalizations and 3,037 people died (Centers for Disease Control 2011). In terms of financial costs, the CDC along with the USDA's Economic Research Service puts the cost of just *Salmonella*-related illnesses at~$2.6 billion in 2009 (USDA/ERS 2010). The latest estimates paint a far worse picture. New data released by The Produce Safety Project at Georgetown University (2010) puts current costs for all food-borne illnesses in the U.S. at ~$151 billion dollars. Given these numbers and the population's awareness of the problem, food-bome pathogen research has become even more important. The National Advisory Committee on Microbiological Criteria for Foods presents an excellent review of food-borne pathogen detection methods from rapid techniques to more traditional standards (National Advisory Committee on Microbiological Criteria for Foods 2010).

Polymerase chain reaction (PCR) assays for bacterial detection is one method that has greatly reduced the time needed for detection. Traditionally, successful amplification of a target gene sequence was confirmed through gel electrophoresis. Modern real-time PCR machines utilize double-stranded DNA binding fluorophores, first developed in the early 1990's (Higuchi et al. 1992; Higuchi et al. 1993). These dyes, such as SYBR green and ethidium bromide, allow scientists to detect amplification of a target sequence as it occurs. This methodology has since been extended to microfabricated devices that allow faster thermocycling times and reduced reagent consumption (Zhang and Xing 2007; Bhattacharya et al. 2008).

However, a portable and fast PCR machine for point-of-care and on-site diagnosis will be limited without a simpler detection method than fluorescence detection of amplified PCR products. As of today, the state of the art microfabricated devices focus mainly on two detection methodologies, (i) an optical detection approach, such as on-chip capillary electrophoresis detection (Woolley et al. 1996; Waters et al. 1998; Huang et al. 2006) or labeling the amplified products with fluorescent dye and reporter particles for detection (Cady et al. 2005; Wang et al. 2006), and, (ii) an electrical approach using either complementary probe binding (Zhang et al. 2010; Ghindilis et al. 2009) or surface charge sensing (Henry et al. 2009; Fritz et al. 2002; Hou et al. 2006; Hou et al. 2007). There have also been many extensive reviews published on the subject of label-free detection (Hunt and Armani 2010; Gooding 2002; Daniels and Pourmand 2007; Park and Park 2009). Although these methods are rapid in comparison to gel electrophoresis, the requirement of an integrated optical component or a functionalized surface for the electrochemical method, not only limits the mobility of such devices, but also increases the labor and total cost of operation.

Instead of using a fluorescence label for optical detection or an oligomeric probe for electrochemical detection, the electrical properties of double stranded DNA molecules (dsDNA) first explored back in 1950's and 1960's (Jerrard and Simmons 1959; Mandel 1961; Takashima 1966) are a good candidate for developing a novel, simpler PCR detection method. In this study, the change in impedance and phase with respect to changing DNA concentration in solution was investigated. By incorporating PCR purification and precipitation, this method was expanded to demonstrate the feasibility of a novel, PCR-based detection method.

2 Method of detection

Double stranded DNA molecules in solution are surrounded by a counter-ion cloud due to their negatively-charged sugar-phosphate backbone (Sakamoto et al. 1976). These counter-ions are usually classified as two layers; one is associated with bound ions, i.e. condensed ions closed to the DNA molecule, while the other layer is a loosely surrounding ion cloud. The two separate counter-ion layers give rise to two different dielectric relaxation points that can be observed when the DNA molecules are probed in an AC electrical field over a range of frequencies (Oosawa 1970; Mandel and Odijk 1984). (Tomic et al. 2007) discussed the mechanisms for the lower frequency dielectric relaxation point in low salt concentrations in great detail. As depicted in Fig. 1, the low frequency dielectric dispersion is thought to be a function of the loosely bound ion cloud fluctuating between the ends of the DNA molecule in an end-to-end movement. As the measurement frequency increases (100 Hz–10 kHz), the dipole formed between the DNA and its surrounding cloud is not able to align with the electric field quickly enough, resulting in a dielectric relaxation point in the system. At higher frequencies (100 kHz–1 MHz), the closely bound condensed ion layer forms a dipole with the negatively-charged phosphate groups of the DNA backbone which introduces another dielectric relaxation point related to the DNA molecule's axial rotation.

In prior work, it was shown that increasing the DNA concentration would increase the effect of the induced dipole moment (Liu et al. 2008a). As the effect of the induced dielectric relaxation point increases and measured impedance and phase of the system changes, it is possible to conclude that the concentration of dsDNA in the system is increasing

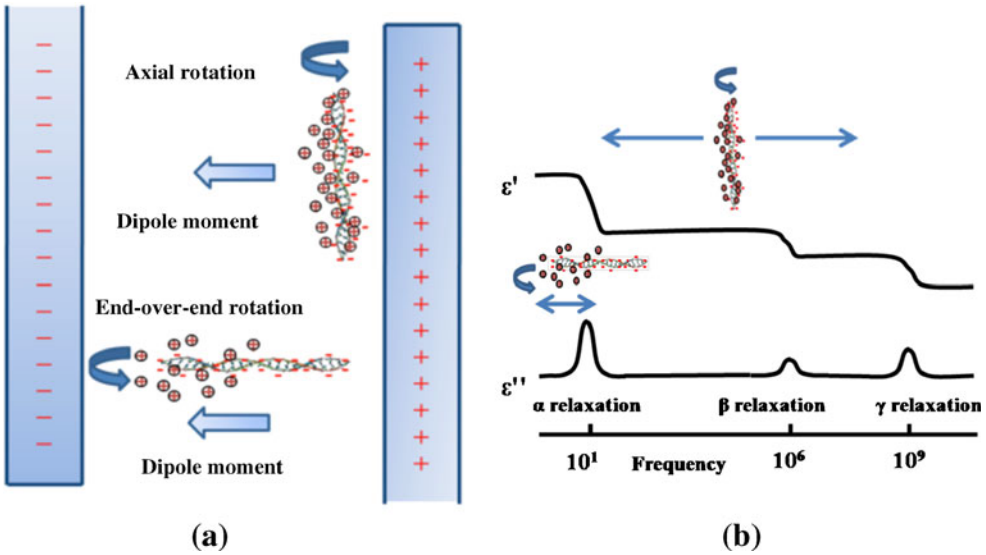

Fig. 1 (**a**) DNA in an AC electric field will generate dipoles whose orientation is frequency dependent. (**b**) Three dielectric relaxation points are known to exist for DNA. The first point is in the low frequency range and corresponds to end-to-end rotation. The second point is in the 100 kHz-1 MHz range and corresponds to axial rotation. The final relaxation point falls above 1 GHz and corresponds to polarizability of water molecules surrounding the DNA molecules (Adapted from Baker-Jarvis et al. 1998)

and that PCR amplification is occurring. However, due to the heterogeneity of the background ions, charge neutralization and tight ion binding to the back-bone in highly ionic solutions (Liu et al. 2008b), as well as noise from included primers, it is necessary to purify and re-suspend the PCR product in deionized (DI) water.

By eliminating the need for optical detection and replacing fluorescence detection with electrical detection of DNA molecules in solution, this paper shows a means to potentially reduce the footprint of a PCR system and still maintain the speed and reliability that food industry quality control demands.

3 Materials

Listeria monocytogenes was cultured in Brain Heart Infusion (BHI) broth from Sigma Aldrich. PBS was also obtained from Sigma Aldrich. Nuclease-free water for the re-suspension of primers and DNA was obtained from Ambion, Inc. Ready-to-go PCR beads were obtained from GE Healthcare Life Sciences. A Qiaquick PCR purification kit from Qiagen, Inc. was used in the preparation of the PCR product. For the DNA precipitation procedure, ammonium acetate, isopropanol, and ethanol were obtained from Sigma Aldrich. The 100, 500, and 5000 bp DNA fragments were purchased from the NoLimits line of DNA at Fermentas Molecular Biology Tools, a division of Thermo Scientific Inc. Primers for the *prfA* gene (Bhattacharya et al. 2008) were purchased from Integrated DNA Technologies, Inc. All centrifugation steps were performed in a Centrifuge 5415D from Eppendorf. DNA sample purity and concentration was interrogated using a Nanodrop spectrophotometer (Nanodrop, Wilmington, DE). Injection of the sample into the microchip was accomplished using a PHD ULTRA syringe pump from Harvard Apparatus. The microchip sensors (see Fig. 2) and LCR meter used were provided by BioVitesse Inc (Sunnyvale, CA).

4 Methods

4.1 DNA precipitation

The 100, 500, 5000 bp DNA molecules were prepared using an isopropanol precipitation method. Briefly, equal volume of ammonium acetate was added to the DNA followed by three times the initial volume of isopropanol. This solution was vortexed on a table-top vortex mixer and then incubated at −20°C for 5 h to ensure precipitation. The samples were then loaded into a centrifuge and centrifuged at room temperature for 25 min at 14000 g. The supernatant was then removed and the tube was washed with 1 mL of 70% ethanol by inverting the tube several times and left to sit on ice for 10 min. The samples were then centrifuged again at 14000 g for 15 min and the ethanol supernatant pipetted off the DNA pellet. The tube was then left to air dry to remove any leftover ethanol for 30 min. Once dry, the DNA molecules were resuspended in nuclease-free DI water and diluted to the desired concentrations. These samples were then centrifuged for 5 min at 14000 g and the supernatant collected. The purity of the DNA samples was confirmed by a spectrophotometer, by examining the A260/A280 ratio, which must fall between 1.8 and 2.0 for pure DNA (Nanodrop, Wilmington, DE).

4.2 PCR samples

All the bacterial DNA samples were prepared from *Listeria monocytogenes* V7 cultures that were incubated for 18–

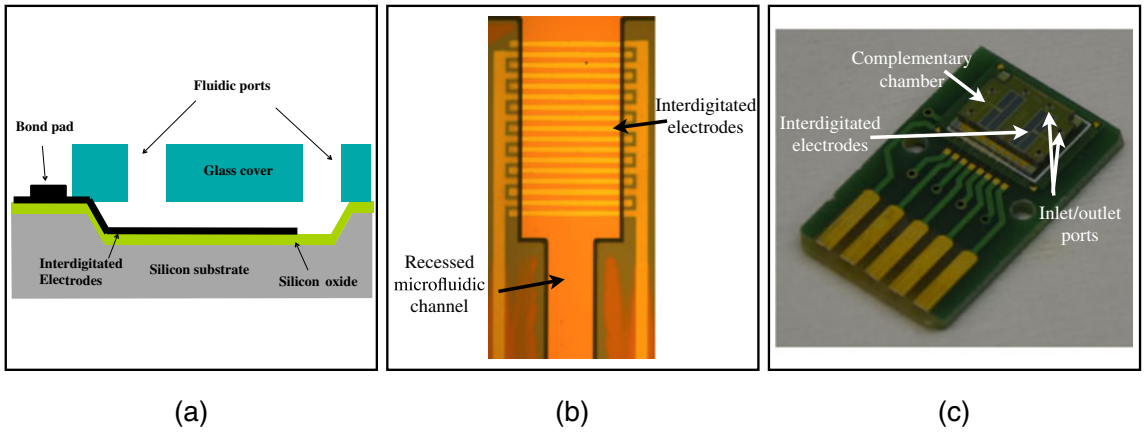

Fig. 2 (**a**) A cross-sectional view of the microchip is shown. The portion containing the interdigitated electrodes comprises a volume of 60 nL. (**b**) A top view of the sensing region is shown. (**c**) The whole chip is shown. Inlet and outlet ports are visible, as well as a secondary sensing chamber that can be used as a reference well

20 h in BHI broth in a 37°C incubator. One mL of cell culture was collected and heat lysed in a 95°C water bath for 15 min, followed by a 5 min quench in a −20°C freezer. Following cell lysis, the cellular debris was spun down at 15000 g for 30 s in a centrifuge. The supernatant was then collected and checked for purities and concentrations by a Nanodrop spectrophotometer (Nanodrop, Wilmington, DE).

PCR amplification was accomplished in triplicate, 25 μL Ready-to-go PCR beads for each reaction. To obtain a view of the reaction kinetics, 0, 20, 30 and 40 cycles were measured. To eliminate pipetting errors between different samples, 16 aliquots of PCR mixture was prepared as follows. Initially 352 μL nuclease free DI water was added to rehydrate the lyophilized beads, followed by 8 μL of 10 μM forward and 8 μL of 10 μM reverse primers to get a final primer concentration of 0.2 μM. Finally, 32 μL of template solution was added to the stock solution. From this point, 75 μL was pipetted into 4 individual tubes for the 0, 20, 30, 40 cycle measurements. Leftover solution was put in a second 40 cycle tube that would be used to confirm successful PCR amplification through gel electrophoresis.

The forward and reverse primers used for the PCR reaction targeted the *L. monocytogenes prfA* gene (508 bp), which encodes a protein that positively regulates *L. monocytogenes* virulence factors:

LMPRFA-F: CGGGATAAAACCAAAACAATTT (5′ to 3′)
LMPRFA-R: TGAGCTATGTGCGATGCCACTT (5′ to 3′)

Samples of designated cycles for each replicate were prepared with all the templates, primers and PCR reagents mixed well before distributing to each PCR reservoir. PCR samples without PCR primers and samples without *Listeria* cell lysate were prepared for all experiments as negative controls to rule out effects from the primers or template DNA alone.

The PCR was performed with a pre-heat step of 94°C for 2 min to ensure the genomic DNA molecules denature to single-stranded DNA. The amplification process consisted of 40 cycles with each cycle containing three steps: 30 s at 94 C for denaturation, 30 s at 55°C for annealing, and 30 s at 72°C for extension. At 0, 20, 30 and 40 cycles, tubes were removed from the PCR thermocycler and placed in a −20°C freezer.

4.3 PCR purification and precipitation

In order to eliminate background noise such as primers, enzymes, cellular debris, and salts, PCR purification was performed using a PCR purification kit from Qiagen. The procedure for this kit can be found in the Qiaquick PCR purification manual. To further purify the amplified DNA and to remove excess salt ions left over from the PCR purification step, an isopropanol precipitation procedure was implemented. This procedure followed the same steps as the precipitation technique that was used with the 100, 500, and 5000 bp DNA samples from Fermentas except that the sample was concentrated to 55 μL from 75 μL and the ethanol washing step was done 1–2 times with 70–95% ethanol.

4.4 Micro-scale device design and fabrication

The biochips were provided by BioVitesse, Inc (Sunnyvale, CA.). The fabrication process of the biochip sensor was similar to Gomez et al. (2001) and started with bare 4″ silicon wafers, with a (100) surface and a thickness of 500 μm. Silicon dioxide was thermally grown on the wafers and subsequently patterned with conventional

photolithography (using Clariant AZ1518 positive photoresist, Clariant Corp.,Somerville, NJ) followed by etching in buffered hydrofluoric acid (BHF). This oxide layer serves as a hard mask for etching the channels in an anisotropic potassium-hydroxide-based etchant to a nominal depth of 12 μm. After etching the channels, the hard mask was removed by etching in BHF and the wafers were thermally reoxidized to create a 2000-Å layer of silicon dioxide. Subsequently, a metal layer, which creates the measurement electrodes and the RTD temperature sensor, was deposited by sputtering 800 Å of platinum over a titanium adhesion layer (Perkin-Elmer Sputterer Model 2400, Perkin-Elmer Inc., Wellesley, MA) and patterned by liftoff. Subsequently, a 10,000-Å-thick layer of gold over a titanium adhesion layer was deposited by electron-beam evaporation (Varian Inc., Palo Alto, CA) and patterned by wet etch to create robust bond-pads. After dicing the wafers, a glass cover was anodically bonded to each die at 400 mAmps with a voltage of 1000 V for 60 min. The glass cover was made from 4″, 500 μm thick polished Pyrex glass wafers type 7740 (Corning Inc., Corning, NY), which were custom diced and ultrasonically drilled to create holes where input/output tubes were attached. The holes in the glass were aligned to the input/output channels in the die before anodic bonding. Figure 2(a) shows a cross section of the packaged device.

After fabrication, each die was fixed onto a custom-designed printed circuit board carrier that allows it to be easily connected to the equipment that measures the impedance, and measures and controls the temperature. The carrier contains an integrated heater and gold-plated bond pads that connect to the pads on the chip by wire bonding. Fig. 2(c) shows a packaged biochip on a pc board.

4.5 Impedance measurement

The LCR meter in the BioVitesse System measured the impedance of each PCR sample. A DI water curve was taken as a baseline reading before each set of measurements to ensure the system had achieved a consistent baseline. After DI, 25 μL of sample solution was injected into the chip at a rate of 20 μL/min. The measurement voltage was

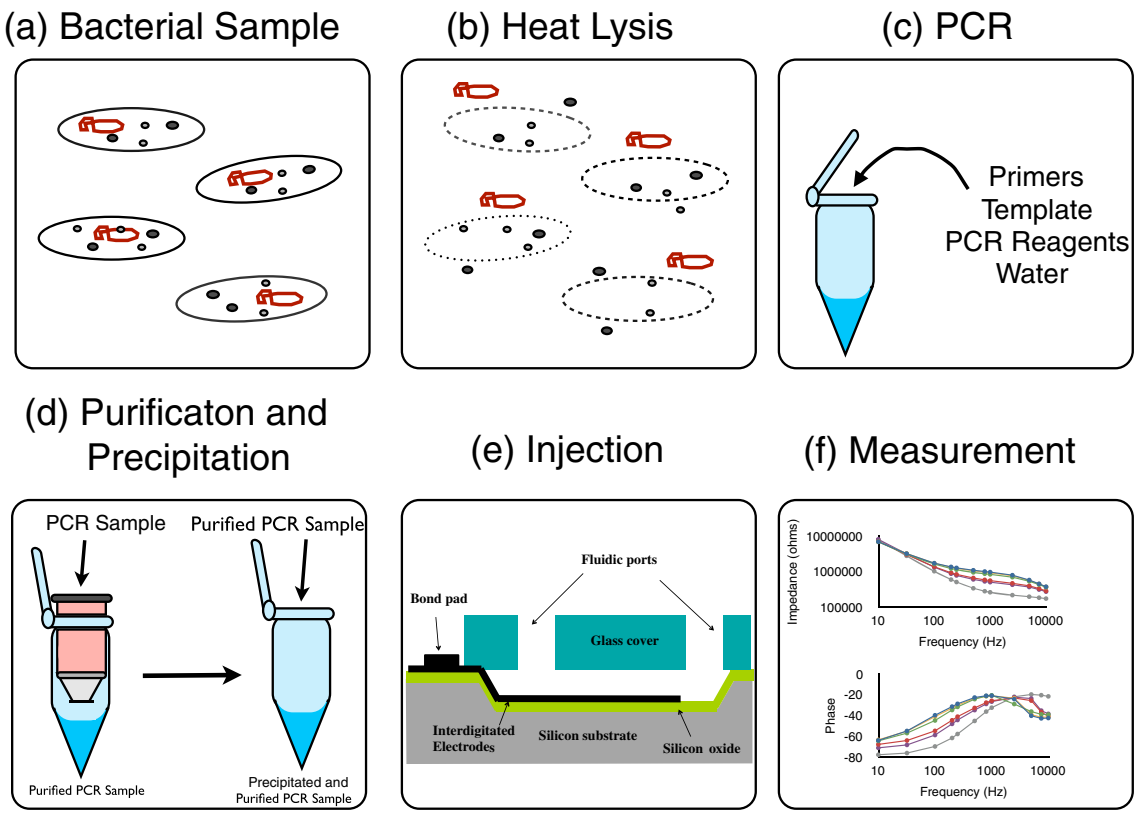

Fig. 3 Schematic depiction of the proposed procedure. Bacterial cells are first cultured in media overnight as depicted in part (**a**). Part (**b**) depicts the cell lysis step, which is done to prepare the cells for PCR. The cell lysate is then mixed with the PCR reagents, primers and DI water as shown in part (**c**). In order to minimize the effects of background noise from excess salts and primers, a post-thermocycling purification and precipitation of the PCR product is performed as shown in part (**d**). Part (**e**) depicts injection of the sample into the microfluidic chip. Once injected in the chip, impedance spectroscopy measurements and subsequent impedance and phase results from the sample are taken as shown in part (**f**)

250 mV_{p-p} with 12 frequencies, 10, 32, 100, 200, 250, 500, 800, 1000, 2500, 5000, 7500, and 10000 Hz. Ten to twelve sweeps were taken for each sample to ensure that the system had stabilized and was functioning properly. To minimize the issue of DNA contamination between cycle samples, the samples were run from low concentration to high concentration or from 0 cycles to 40 cycle. The overall PCR detection scheme outlined above is shown in Fig. 3.

4.6 PCR confirmation

As a method of amplification confirmation, gel electrophoresis was run for each cycle sample with a 100 bp DNA ladder from BioRad as the standard. The 100 mL gel was made with 1×TE buffer, 1% high purity agarose and 2 μL ethidium bromide. The samples were loaded into the wells using a loading dye from BioRad. The gel was then run at 100 V for approximately 2 h. An image of the gel was taken using a GelDoc XR system with a UV transilluminator (BioRad).

5 Results/discussion

5.1 Varying DNA molecule length and concentration in DI water

The impedance spectroscopy plots for the 100, 500, and 5000 bp samples from Fermentas are shown in Fig. 4. It can

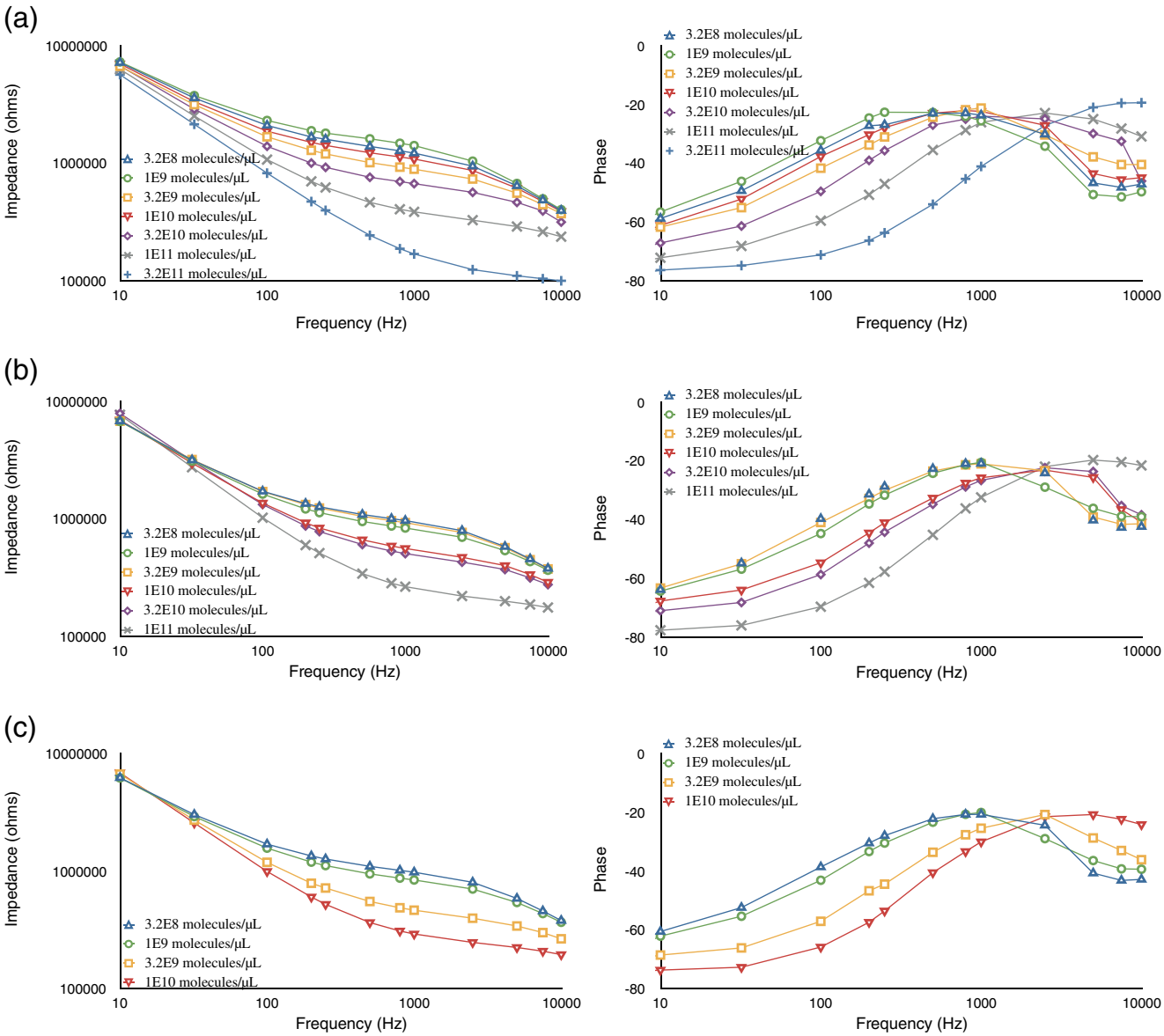

Fig. 4 Pure DNA samples diluted in nuclease free DI water were tested. The above figure shows (**a**) 100, (**b**) 500, and (**c**) 5000 bp DNA fragments as they were interrogated from 10 Hz–10 kHz. Changes in phase and impedance can be seen with varying DNA concentration

be seen that as the concentration of DNA molecules increases for 100, 500, and 5000 bp, the impedance decreases and the dielectric relaxation point shifts to higher frequencies.

The change in impedance can be attributed to the increasing number of molecules in solution and the resulting change in capacitance and conductivity. The shifting relaxation point is more difficult to understand. As the number of molecules increases, the dielectric relaxation point shifts to higher frequencies. This implies that the time it takes for dipole formation is shorter. There are two likely reasons for this phenomenon. For DNA strands in lower salt concentration solutions, the persistence length of the DNA molecule will decrease with increasing solution conductivity and salt concentration (Hagerman 1988). In Fig. 5(a), the increase in the conductivity of the solution can also be seen in the changing impedance values for the different length DNA molecules at 1 kHz. As the persistence length decreases, the degree of coiling of the DNA molecule will increase. This leads to a decreased effective length of the molecule, which will allow the counter-ion cloud and dipole alignment to occur at higher frequencies. A secondary effect arises from the changing concentration of DNA. Dobrynin and Rubinstein (2005) were able to show that the number of condensed counter-ions increases with increasing polyelectrolyte concentration. As the number of condensed counter-ions increases, electrostatic interactions in the DNA chain are weakened. Weakening of the repulsive forces between negatively-charged phosphate groups causes shrinkage in the polyelectrolyte chain. By reducing the length of the polyelectrolyte chain, counter-ion cloud and dipole alignment can happen at a quicker rate which shifts the relaxation point to a higher frequency, a result that is repeated in our work and is especially applicable to the 100 bp sample whose chain length is less than the average persistence length of DNA.

5.2 Detection of PCR amplification

After establishing the detection limit of dsDNA molecules in DI water, we applied the label-free impedance spectroscopy method to detection of PCR amplification. In order to minimize the effects of excess primers, charge shielding, ion binding, and variance in ion composition, the amplified PCR product was first purified to remove primers and PCR reagents and then precipitated out of solution and re-suspended in DI water in order to remove excess salt ions.

Figure 6 shows the raw data from one of the sample runs consisting of a full PCR sample, a sample lacking template DNA (primer only) and a sample lacking primers (template only). An increase in the relaxation maxima from 0 to 40 cycles in the full PCR sample can be seen in the raw data. As confirmed through gel electrophoresis (Fig. 7) and nanodrop spectrophotometery, the 40 cycle sample contained roughly 1×1011 508 bp molecules/μL. This is similar to the highest 500 bp concentration studied in the dsDNA test from Fig. 4 (b). Results from the full PCR test are consistent with the 500 bp dsDNA test. To confirm the increase in relaxation maxima in the phase is solely due to the amplified PCR product, two negative controls, primer only and template only, were also measured. The primer only sample showed no increase in relaxation maxima and no decrease in impedance from 0 to 30 cycles. However a slight decrease can be seen in the 40 cycle measurement. This shift could be due to the non-specific generation of primer dimers. It was expected that through the purification procedure, these dimers would be removed; however, it is clear that the purification step is not 100% efficient for primer dimer removal. The template only sample showed no appreciable change from 0 to 40 cycles as expected. Figure 7 depicts a slightly more complex view of this electrical characterization system. Inconsistencies in preparation and washing steps resulting in variability in the removal of salts can lead to large shifts in the measured impedance and phase data

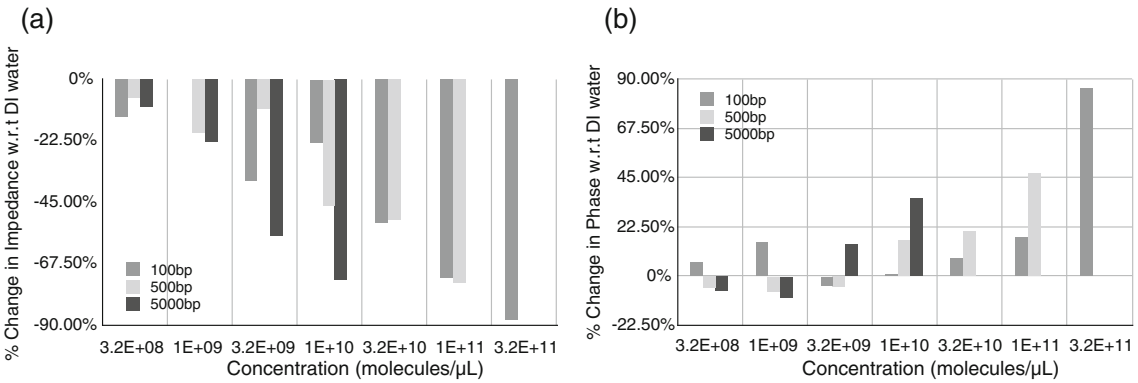

Fig. 5 (**a**) The change in impedance at 1 kHz referenced to a DI sample is shown. It can be seen that the change in impedance shows concentration dependence within each sample. Between each sample it can be seen that there exists a dependence on molecular weight. (**b**) Trend with a phase measurement that has been referenced to a DI sample

between experiments. Specifically, the impedance data (not shown) across multiple samples showed varied results that were not statistically different. Great care was taken in preparation of these samples; however, the importance of standardizing the washing technique in order to limit human error cannot be overstated for this approach. However, as can be seen in Fig. 7(a), the percent change in phase relative to the 0 cycle measurements is a reliable indicator of PCR amplification. To demonstrate statistical significance of the difference between positive amplification and the negative controls, a one-way analysis of variance (ANOVA) test was performed. Although the 20 and 30 cycle measurements showed no statistically significant difference; the 40 cycle measurement had a p-value<0.01. This shows that the results at 40 cycles are statistically significant enough to allow differentiation between the positive and negative control samples.

The amount of target DNA at 40 cycles is consistent with our projected detection limit from the dsDNA in DI

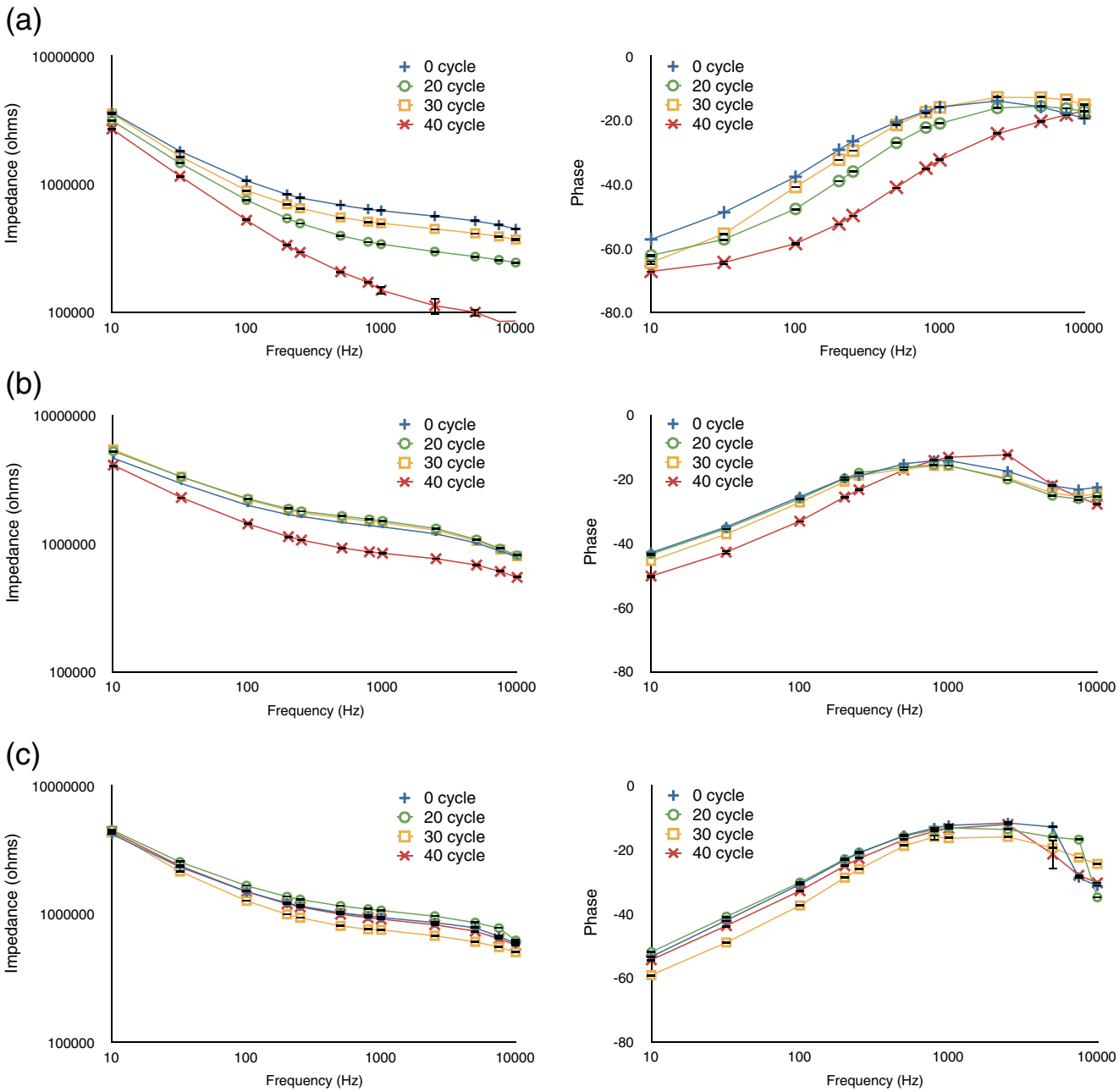

Fig. 6 Purified PCR samples were tested over a range of 10 Hz–10 kHz. The impedance and phase response is charted for (**a**) a full PCR test, (**b**) a primer only test, and (**c**) a template only test. In each test, different thermocycling points ranging from 0 cycles up to 40 cycles are measured in order to monitor the change in impedance and phase relative to target DNA concentration

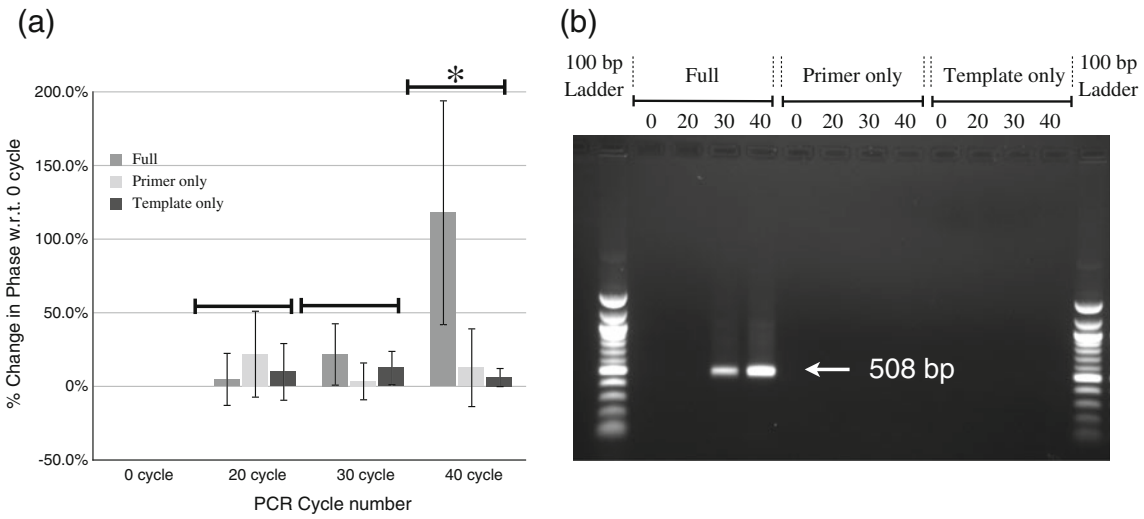

Fig. 7 The percent change in phase (**a**) was plotted with respect to the 0 cycle measurement. Using a one-way ANOVA test, the difference between the 20 and 30 cycle measurements is not statistically significant; however, the difference between the 40 cycle samples is statistically significant. The asterisk indicates a sample set with a *p*-value<0.01. Gels were run for each sample to confirm amplification. An example gel is shown in (**b**)

tests, 1×1011 molecules/μL. From a theoretical standpoint, this level of molecules/μL is possible at 40 cycles when starting from around 7 copies of template DNA per 75 μL reaction volume. Also, factoring in reagent limitations from the PCR solution's 200 μM dNTP mix, this experiment's max yield was ~1.7×1011 molecules/μL, which is still above our expected detection limit. Therefore, given the yield and the PCR amplicon recovery from purification and precipitation are maximized, this methodology could allow for a detection limit of around 100 CFU/mL. Nevertheless, a system that requires 40 cycles to allow reasonable accuracy in determining PCR amplification exceeds the number of thermal cycles typically desired. Above 30–35 cycles, concerns of primer dimers and non-specific amplification become an issue. This detection limit would have to be lowered. The best option for this improvement would be to improve the consistency of the washing procedures thereby removing unavoidable human-error during pipetting and mixing in the isopropanol precipitation procedure. Possible next steps include on-chip capture of the amplified molecules and subsequent washing and exchange of salt solutions.

6 Conclusions

This study details our efforts toward development of a label-free, PCR biosensor capable of detecting changing DNA concentration. While the current detection limit of this system is relatively high, in the 30–40 cycle range, further development of the system could put its capabilities on par with current real-time PCR detection devices. Amplifying the signal from the DNA molecules is a strong possibility for improvement. This can either be done through concentration of the DNA at the electrode surface through a technique such as dielectrophoresis (Asbury et al. 2002) or through inclusion of negatively-charged DNA binders (Kafka et al. 2008). Another key component to enhance in this system would be to limit off-chip procedures. There have been reports of integrating PCR purification into a microfluidic device (Wolfe et al. 2002; Cady et al. 2003; Wen et al. 2008, Min et al. 2011). By combining an on-chip thermocycling process and a PCR purification step with electrical detection of DNA molecules, an on-site diagnostic system with minimal cost and footprint is possible.

Overall, this study has laid down the basis for a label-free electrical detection method for PCR on chip. We confirm the importance of background ions and salts in these measurements and show that they have to be removed from the sample before electrical measurements are to be performed. In the future, this technique could be incorporated into a lab-on-a-chip device and used as a point-of-care diagnostic device for the food industry or for medical applications.

Acknowledgements We acknowledge funding support from a cooperative agreement with Purdue University and the Agricultural Research Service of the United States Department of Agriculture, project number 1935-42000-035, and a sub-contract to the University of Illinois at Urbana-Champaign.

References

C.L. Asbury, A.H. Diercks, G. van den Engh, Electrophor **23**, 2658–2666 (2002)

J. Baker-Jarvis, C. A. Jones and B. Riddle, NIST Tech. Note 1509, (1998)

S. Bhattacharya, S. Salamat, D. Morisette, P. Banada, D. Akin, Y.-S. Liu, A.K. Bhunia, M. Ladisch, R. Bashir, Lab. Chip **8**, 1130–1136 (2008)

N.C. Cady, S. Stelick, C.A. Batt, Biosens Bioelectron **19.1**, 59–66 (2003)

N.C. Cady, S. Stelick, M.V. Kunnavakkam, C.A. Batt, Sens Actuators B **107**, 332–341 (2005)

Centers for Disease Control, "Centers for Disease Control. "CDC—Estimates of Foodborne Illness Questions and Answers." Updated 19 Apr. 2011. Accessed 05 May 2011 <http://www.cdc.gov/foodborneburden/questions-and-answers.html>

S.R. Crutchfield, T. Roberts, Food Rev **23.3**, 44–49 (2000)

J.S. Daniels, N. Pourmand, Electroanal. **19.12**, 1239–1257 (2007)

A. Dobrynin, M. Rubinstein, Progr. Polym., Sci. **30.11**, 1049–1118 (2005)

J. Fritz, E.B. Cooper, S. Gaudet, P.K. Sorger, S.R. Manalis, PNAS **99.22**, 14142–14146 (2002)

A.L. Ghindilis, M.W. Smith, K.R. Schwarzkopf, C. Zhan, D.R. Evans, A.M. Baptista, H.M. Simon, Electroanal. **21.13**, 1459–1468 (2009)

R. Gomez, R. Bashir, T. Geng, A. Bhunia, M. Ladisch, H. Apple, S. Wereley, Biomed. Microdevices **3.3**, 201–209 (2001)

J.J. Gooding, Electroanal **14.17**, 1149–1156 (2002)

P.J. Hagerman, Annu Rev Biophys Biophys Chem **17.1**, 265–286 (1988)

O.Y.F. Henry, J.L. Acero Sanchez, D. Latta, C.K. O'Sullivan, Biosens Bioelectron **24.7**, 2064–2070 (2009)

R. Higuchi, G. Dollinger, P.S. Walsh, R. Griffith, Biotech **10.4**, 413–417 (1992)

R. Higuchi, C. Fockler, G. Dollinger, R. Watson, Biotech **11.9**, 1026–1030 (1993)

C.J. Hou, N. Milovic, M. Godin, P.R. Russo, R. Chakrabarti, S.R. Manalis, Anal Chem **78**, 2526–2531 (2006)

J. Hou, M. Godin, K. Payer, R. Chakrabarti, S.R. Manalis, Lab Chip **7**, 347–354 (2007)

F.-C. Huang, C.-S. Liao, G.-B. Lee, Electrophor **27**, 3297–3305 (2006)

H.K. Hunt, A.M. Armani, Nanoscale **2**, 1544–1559 (2010)

H.G. Jerrard, B.A.W. Simmons, Nature **184**, 1715–1716 (1959)

J. Kafka, O. Panke, B. Abendroth, F. Lisdat, Electrochimica Acta **53.25**, 7467–7474 (2008)

Y-S. Liu, P.P. Banada, A.K. Bhunia and R. Bashir, Proc. IEEE Sens., art. no. 4716498, 550–553, (2008)

Y.-S. Liu, P.P. Banada, S. Bhattacharya, A.K. Bhunia, R. Bashir, Appl Phys Lett **92.14**, 143902 (2008b)

M. Mandel, Mol Phys **4.6**, 489–496 (1961)

M. Mandel, T. Odijk, Annu Rev Phys Chem **35.1**, 75–108 (1984)

J. Min, J.-H. Kim, Y. Lee, K. Namkoong, H.-C. Im, H.-N. Kim, H.-Y. Kim, N. Huh, Y.-R. Kim, Lab Chip **11**, 259–265 (2011)

National Advisory Committee on Microbiological Criteria for Foods, J. of Food Prot **73.6**, 1160–1200 (2010)

F. Oosawa, Biopolym **9.6**, 677–688 (1970)

J.-Y. Park, S.-M. Park, Sensors **9.12**, 9513–9532 (2009)

M. Sakamoto, H. Kanda, R. Hayakawa, Y. Wada, Biopolym **15.5**, 879–892 (1976)

R.L. Scharff, The Produce Safety Report Project at Georgetown University. 3 Mar. 2010. Accessed 12 June 2011. <http://www.producesafetyproject.org/media?id=0009>

S. Takashima, J Phys Chem **70.5**, 1372–1380 (1966)

S. Tomić, S. Dolanski Babić, T. Vuletić, L. Griparić and R. Podgornik, Phys. Rev. E, 75.2, art. no. 021905, (2007)

United States Department of Agriculture. "ERS/USDA Data Foodborne Illness Cost Calculator." USDA Economic Research Service—Home Page. Updated 28 Dec. 2010. Accessed 03 Apr. 2011. <http://www.ers.usda.gov/data/foodborneillness/>

J. Wang, Z. Chen, P.L.A.M. Corstjens, M.G. Mauk, H.H. Bau, Lab Chip **6.1**, 46–53 (2006). doi:46

L.C. Waters, S.C. Jacobson, N. Kroutchinina, J. Khandurina, R.S. Foote, J.M. Ramsey, Anal Chem **70**, 5172–5176 (1998)

J. Wen, L.A. Legendre, J.M. Bienvenue, J.P. Landers, Anal Chem **80.17**, 6472–6479 (2008)

K.A. Wolfe, M.C. Breadmore, J.P. Ferrance, M.E. Power, J.F. Conroy, P.M. Norris, J.P. Landers, Electrophor **23.5**, 727–733 (2002)

A.T. Woolley, D. Hadley, P. Landre, A.J. deMello, R.A. Mathies, M. Allen Northrup, Anal. Chem **68**, 4081–4086 (1996)

C. Zhang, D. Xing, Nucl. Acids Res **35.13**, 4223–4237 (2007)

G. Zhang, L. Zhang, M.J. Huang, Z.H.H. Luo, G.K.I. Tay, E.A. Lim, T.G. Kang, Y. Chen, Sens. and Actuators, B: Chemical **146.1**, 138–144 (2010)